

# ON PERIODIC FUNCTIONS AS REGULARIZERS FOR QUANTIZATION OF NEURAL NETWORKS

**Maxim Naumov, Utku Diril, Jongsoo Park,  
Benjamin Ray, Jędrzej Jablonski and Andrew Tulloch**  
Facebook, 1 Hacker Way, Menlo Park, CA, 94025

## ABSTRACT

Deep learning models have been successfully used in computer vision and many other fields. We propose an unorthodox algorithm for performing quantization of the model parameters. In contrast with popular quantization schemes based on thresholds, we use a novel technique based on periodic functions, such as continuous trigonometric sine or cosine as well as non-continuous hat functions. We apply these functions component-wise and add the sum over the model parameters as a regularizer to the model loss during training. The frequency and amplitude hyper-parameters of these functions can be adjusted during training. The regularization pushes the weights into discrete points that can be encoded as integers. We show that using this technique the resulting quantized models exhibit the same accuracy as the original ones on CIFAR-10 and ImageNet datasets.

## 1 INTRODUCTION

Deep learning models require a very large amount of resources during their training (repeated forward and backward propagation) as well as inference (forward propagation). Further, the latter is often performed on the edge devices, such as smartphones or embedded systems, which operate within strict size, temperature and power budget Shimpi (2011); Humrick (2017); Dolbeau (2018); NVIDIA (2018). As a result these devices can perform a limited # of operations per second<sup>1</sup>, as illustrated in Tab. 1.

CPU/GPU	GHz	Watts	fp32	fp16	int8
ARM Cortex A-7 (2-core)	1.5	1.5	3	†	12
ARM Cortex A-75(4-core)	3.0	4	48	96	96
NVIDIA Turing Tesla T4	1.35	70	8100	16200	130000

Table 1: Peak GFlops/Gops according to specification

In order to decrease the storage and compute requirements of the model during inference its parameters are often stored as integers with a low number of bits. It is common to use 8-bit integers (1 Byte), rather than 16- (2 Bytes) or 32-bit (4 Bytes) floating point numbers. The process of converting model parameters from “continuous” floating point to discrete integer numbers is called quantization.

Let the original optimization problem be

$$\min_w L(w, x) \quad (1)$$

where  $L$  is the loss measured during training. There are many different quantization schemes based on symmetric vs. asymmetric intervals, uniform vs. non-uniform discrete partitioning, different rounding modes and choices for handling the outliers, e.g. few elements that lie outside of the range of most of the other elements.

<sup>1</sup>The peak for ARM Cortex is based on fp32 “VMLA.F32 Qd, Qn Dm”, fp16 “VMLA.F16 Qd, Qn Dm” and int8 “VMLAL.S8 Qd, Dn, Dm” instructions, with estimated reciprocal throughput 4, †, 2 and width 4, †, 8 for A-7, reciprocal throughput 1, 1, 1 and width 4, 8, 8 for A-75. Then, peak ops are defined as (frequency/throughput)\*width\*cores. Also, the power is assumed to be 750mW and 1W per core for ARM Cortex A-7 and A-75, respectively.

Let us consider a uniform quantization of the parameter weights  $W = [w_{ij}]$ , for example from the either convolution (14) or fully connected layers (15), and activations. Then, the quantized problem is commonly written as

$$\min_w L(Q(w), Q(x)) \quad (2)$$

where  $Q$  is the quantization function.

For instance, if we use only two intervals then the process is referred to as binarization and resulting element can be stored in a single bit Courbariaux et al. (2015; 2016); Hubara et al. (2018); Rastegari et al. (2016). It can be performed using a single threshold point  $\epsilon$  as shown below

$$Q(w) = \begin{cases} -1 & \text{if } w < \epsilon \\ +1 & \text{otherwise} \end{cases} \quad (3)$$

The ternary networks use three intervals with resulting elements stored in 2 bits Li et al. (2016); Mellempudi et al. (2017); Choi et al. (2018). Then, quantization can be performed using two threshold points  $\epsilon_1$  and  $\epsilon_2$  resulting in

$$Q(w) = \begin{cases} -1 & \text{if } w < \epsilon_1 \\ 0 & \text{if } \epsilon_1 \geq w \geq \epsilon_2 \\ +1 & \text{if } w > \epsilon_2 \end{cases} \quad (4)$$

Finally, let arbitrary # of bits  $t$  correspond to  $2^t$  points and  $2^t + 1$  intervals. Let us assume that we would like to quantize floating point number  $w \in [a, b]$ , with  $c = \max(|a|, |b|)$  and length  $d = (b - a)/2$ . A uniform quantization can be performed symmetrically in the interval  $[-c, c]$  using multiplier  $\gamma = c/(2^{t-1} - 1)$ , so that

$$Q(w) = \gamma * \text{round}(w/\gamma) \quad (5)$$

with  $2^t - 1$  effective points because 0.0 is double counted.

On the other hand, notice that we can shift the interval  $[a, b]$  to the interval  $[-d/2, d/2]$  located around 0.0 by adding a scalar bias term  $s = (a + b)/2$ . Therefore, uniform asymmetric quantization can be performed with bias  $s$  using multiplier  $\delta = d/(2^t - 2)$ , so that

$$Q(w) = \delta * \text{round}((w - s)/\delta) + s \quad (6)$$

where `round` operation rounds a floating point to an integer value Wen et al. (2016); Jacob et al. (2017); Krishnamoorthi (2018).

The advantage of symmetric quantization is that for sparse parameters, with a lot of 0.0 elements, the sparsity is preserved. Note that computation with zeroes can be skipped in hardware Albericio et al. (2016); Venkatesh et al. (2016); Reagen et al. (2016); Chen et al. (2017); Kim et al. (2017); Parashar et al. (2017). The disadvantage is that for highly asymmetric intervals many discrete representations may be wasted.

The non-uniform quantization assigns discrete points to the interval based on the distribution of floating point values in it Bagherinezhad et al. (2017); Wang et al. (2018). Therefore, it does not have a fixed stride from one point to the next. Its advantage is that the encoded values are more representative of the original ones, but at the same time it can be hard to map back and perform operations with them.

The techniques for handling outliers and determining maximum thresholds, e.g. using adaptive schemes, KullbackLeibler (KL) divergence measured loss of information, or L2 error minimization in Caffe2, have been investigated in Jia et al. (2014); Migasz; Zhou et al. (2017); Park et al. (2018).

However, independent of all of these choices, notice that a common trend among (3) - (6) is that fixed thresholds are used in quantization function  $Q$  to clamp floating point values to discrete points. We point out that the matrix- and neural network-based compression techniques are outside the scope of this paper Gong et al. (2014); Denton et al. (2014); Jaderberg et al. (2014); Mishra & Marr (2018).

In this paper we will focus on a very different approach for uniform quantization using periodic functions, such as trigonometric sine (or cosine) as well as hat functions. We discuss uniform quantization, but our ideas can be generalized to non-uniform case using variations of these periodic functions with decaying amplitude and increasing base lengths away from the origin Stenger (1993); Strang & Fix (2008).

## 2 PERIODIC FUNCTIONS AS REGULARIZERS

We propose an unorthodox approach for quantizing the weights of a neural network. Instead of using quantization function  $Q$ , we propose adding a regularization term  $R$  to the loss, so that the resulting optimization problem is written as

$$\min_w L(w, x) + \lambda R(w, x) \quad (7)$$

where  $\lambda$  is a scalar scaling parameter.

The regularization term  $R$  is a sum of periodic functions that push the values of the weights (and potentially activations) to a set of discrete points during training. Next we will discuss different choices for these functions.

### 2.1 TRIGONOMETRIC (CONTINUOUS) FUNCTIONS

Let us focus only on the weights and use trigonometric sine, so that

$$R(w) = \sum_{\forall w} \text{amplitude} * \sin^2(\pi * \text{frequency} * (w/c)) \quad (8)$$

where  $c$  is the maximum weight in absolute value as defined in (5).

Notice that for frequency=1 the function  $R(w)$  attains its minimum 0.0, when the weight values are distributed at 3 discrete locations, while for frequency=7 it attains its minimum 0.0, when the weight values are distributed at 15 discrete locations, as shown on Fig. 1a and 1b, respectively.

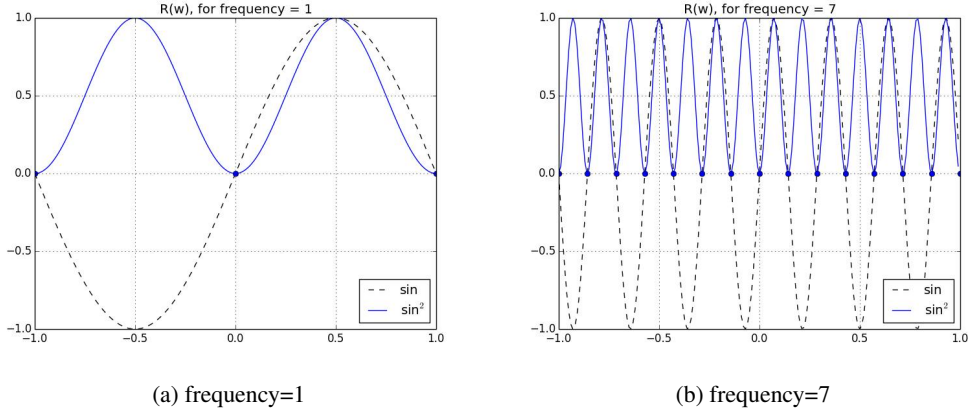


Figure 1: Plot of sine and its square for amplitude=1

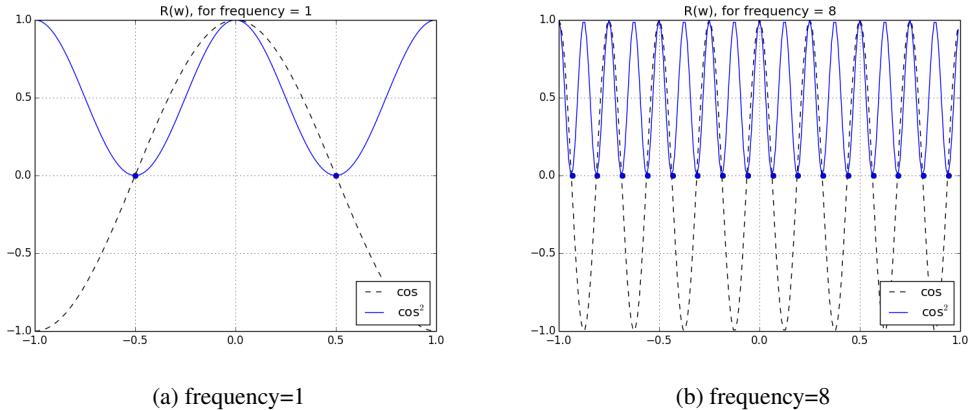


Figure 2: Plot of cosine and its square for amplitude=1

An analogous plot can also be created using a trigonometric cosine function and its square, with a difference being a shift in the discrete points so that there are 16 rather than 15 of the points where minimum is attained, but perhaps most importantly 0.0 is not preserved, see Fig. 2a and 2b.

## 2.2 HAT (NON-CONTINUOUS) FUNCTIONS

Let us focus only on the weights and use a hat function, so that

$$R(w) = \sum_{\forall w} \text{amplitude} * |((\text{frequency} * ((w/c) - 0.5)) \% 1) * 2 - 1| \quad (9)$$

where  $c$  is the maximum weight in absolute value as defined in (5).

Once again, notice that for frequency=1 the function  $R(w)$  attains its minimum 0.0, when the weight values are distributed at 3 discrete locations, while for frequency=7 it attains its minimum 0.0, when the weight values are distributed at 15 discrete locations, as shown on Fig. 3a and 3b, respectively. Here we show variant of the hat function corresponding to sine, while a shifted variant corresponding to cosine is also possible.

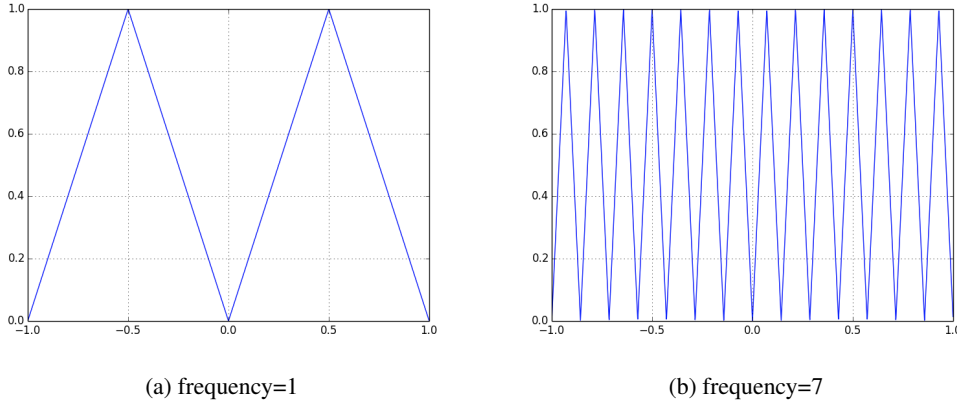


Figure 3: Plot of hat for amplitude=1

Notice that the use of regularization for the purpose of quantization has been suggested in Hung et al. (2015). However, in this earlier work the authors use distance from fixed points (centroids)  $q$  as a penalty measure to ensure quantization. This contrasts with our periodic trigonometric sine and hat functions, with amplitude and frequency hyper-parameters defined in (8) and (9), respectively.

It is important to highlight a few differences between sine (or cosine) and hat functions. Notice that sine function has very nice properties. It is periodic, continuous and differentiable. However, it is not convex, unlike many of the existing regularizers. Also, notice that the maximum value of the regularizer  $R(w)$  is known ahead of time. It can be computed by assuming that all weights translate into value 1.0 after application of the  $\sin^2$  function. Then, the regularizer can be scaled by a constant  $\gamma$ , such that  $\gamma R(w) \in [0, 1]$ . This can be used to facilitate and in fact define the regularizer scaling  $\lambda$  in (7), therefore reducing the number of hyper-parameters.

Also, sine function has a gradient that is zero (or close to zero) in the neighborhood of points where it attains its minimum and maximum values. This property might make escaping the maximum or approaching the minimum slow in their respective neighborhoods. On the other hand, hat function is non-convex and non-continuous, with constant gradient towards the minimum except for the points where it attains its minimum and maximum values, where the gradient does not exist. These trade-offs might guide the choice between these functions, in a way similar to that of a choice between Sigmoid and ReLU activation functions.

Finally, notice that amplitude can be changed adaptively during the training procedure, which allows us to obtain higher test accuracy, as will be shown in the experiments section. The frequency can also be varied during training, but these experiments are outside of the scope of this paper.

---

### 2.3 FROM BITS TO FREQUENCY AND VICE-VERSA

In practice we are interested in selecting the number of bits  $t$  to be used for quantization. For the sine and associated hat function the frequency corresponding to  $t > 1$  number of bits can be found by using

$$\text{frequency} = 2^{t-1} - 1 \quad (10)$$

and vice-versa

$$t = \lceil \log_2(\text{frequency} + 1) + 1 \rceil \quad (11)$$

so that frequency 1 implies 2 bits, while frequency 7 implies 4 bits.

On the other hand, for cosine the frequency corresponding to  $t > 0$  number of bits can be found by using

$$\text{frequency} = 2^{t-1} \quad (12)$$

and vice-versa

$$t = \lceil \log_2(\text{frequency}) + 1 \rceil \quad (13)$$

For instance, frequency 1 implies 1 bit, while frequency 8 implies 4 bits, and so on and so forth.

## 3 EXPERIMENTS

In this section we will investigate the accuracy of ResNet-20 on CIFAR-10 and ResNet-50 on ImageNet datasets He et al. (2015); Krizhevsky et al. (2009); Deng et al. (2009). We will compare the test error achieved by the original and quantized models with loss function defined in (1) and (7), respectively. The regularization term we add to the loss in (7) relies on periodic functions: trigonometric sine in (8) and hat in (9). It can be computed using the following PyTorch Paszke et al. (2017) code snippet

```
def periodic_regularization(model, amplitude, frequency):
    pi = 3.141592
    total = 0
    for m in model.modules():
        if isinstance(m, nn.Conv2d) or isinstance(m, nn.Linear):
            ic = 1/w.abs().max()
            rw = torch.sum(amplitude *
                #either sin
                torch.pow(torch.sin(pi * frequency * (w * ic)), 2))
            #or hat function
            torch.abs((((w * ic) - 0.5) * frequency) % 1) * 2 -1))
```

The training is performed using batch size 256 with default 100 epochs for CIFAR-10 and 90 epochs for ImageNet dataset. We use a fixed schedule that adjusts the amplitude hyper-parameter every 30 epochs. We start with a small amplitude, such as  $10^{-4}$ , and progressively adjust it until it reaches, say  $10^{-1}$  after typical 100 epochs of training. Notice that amplitude subsumes the scaling hyper-parameter  $\lambda$ , which is always set to 1.0. Note that other than using a fixed schedule we do not require any special treatment for the first or last model layers or training epochs, which is otherwise often required to produce good approximations. We show the results of representative runs.

After training the model is quantized using symmetric uniform quantization in (5), which can be performed using the following PyTorch Paszke et al. (2017) code snippet

```
def quantize_model(model, frequency):
    def quantize_weights(m):
        if isinstance(m, nn.Conv2d) or isinstance(m, nn.Linear):
            c = m.weight.abs().max().data
            m.weight.data.mul_(frequency/c)
            m.weight.data.round_()
            m.weight.data.mul_(c/frequency)

    model.apply(quantize_weights)
```

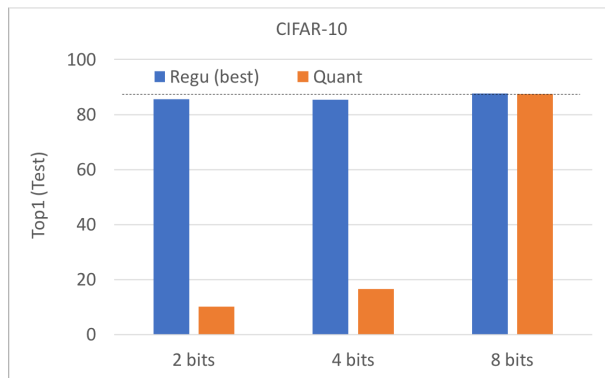


Figure 4: Plot of Top1 test error for CIFAR-10 dataset with Resnet20

We illustrate the difference between original, original with regularization (Regu), and quantized model (Quant) for CIFAR-10 dataset on Fig. 4. The accuracy of the original model is plotted with a black dotted line, while the accuracy of other models is plotted with color bars. Notice that the model accuracy changes significantly depending on the number of bits used for quantization. For instance, there seems to be a clear boundary between 4 and 8 bits, where there seems to be (not or) enough bits to represent the information. Notice that while the training succeeds in all cases, the quantization fails to produce accurate results with less than 8 bits.

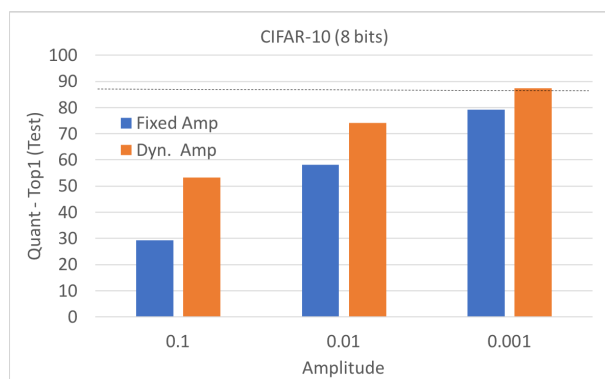


Figure 5: Plot of Top1 test error for CIFAR-10 dataset with Resnet-20

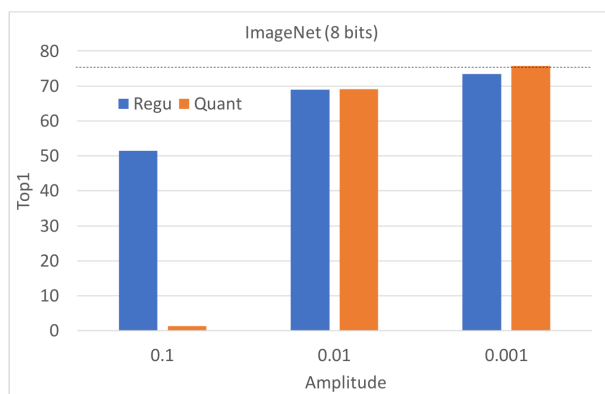


Figure 6: Plot of Top1 test error for ImageNet dataset with Resnet-50

Also, we illustrate the attained model accuracy with different starting amplitudes for CIFAR-10 dataset on Fig. 5. The accuracy of the original model is plotted with a black dotted line, while the

accuracy of the 8-bit quantized model is plotted with color bars. Notice that using adaptive rather than static amplitude allows us to reach higher test accuracy. Also, in our experiments we have found that it is a good practice to target the initial amplitude and choice of fixed schedule such that the final amplitude is in the range of 0.01 - 0.001, which would correspond to a reasonable value of the regularization scaling  $\lambda$ . We observe similar results on the ImageNet dataset, as seen on Fig. 6.

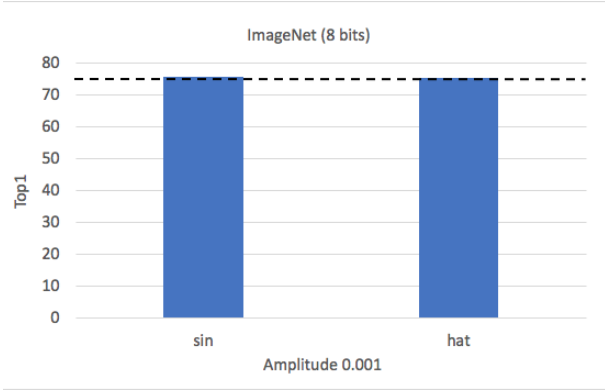


Figure 7: Plot of Top1 test error for ImageNet dataset with Resnet-50

Finally, notice that both sine and hat functions perform as well on the ImageNet dataset, as shown in Fig. 7. Once again, the accuracy of the original model is plotted with a black dotted line, while the accuracy of the 8-bit quantized model is plotted with color bars. In all plots, amplitude denotes the final amplitude. The detailed results are also summarized in tables Tab. 2 and 3.

	Default Model test (best)	Quantized model (with sine)				
		8 bits			4 bits	2 bits
Amplitude	n/a	0.1	0.01	0.001	0.001	0.001
Test error (fixed)	84.72 (87.70)	29.26	58.18	79.18	n/a	n/a
Test error (dyn)	84.72 (87.70)	53.28	74.14	87.46	16.66	10.20

Table 2: CIFAR-10: summary of representative experiments

	Default Model	Quantized model (with sine)			(with hat)
		8 bits			8 bits
Amplitude	n/a	0.1	0.01	0.001	0.001
Top1 error	75.84	1.29	69.02	75.77	75.57
Top5 error	92.90	4.62	89.27	92.54	92.58

Table 3: ImageNet: summary of representative experiments

## 4 CONCLUSION AND FUTURE WORK

We have proposed a novel technique for quantizing neural networks, based on regularization with periodic functions. We have shown that it can be effectively used to quantize ResNets on CIFAR-10 and ImageNet datasets. In our experiments we have achieved virtually no losses vis--vis standard model by using amplitude scaling on a fixed schedule through training followed by 8-bit integer quantization. While similar quality results exist for quantization of CNNs, in this note we have achieved them through a completely novel method. In the future, we would like to incorporate the quantization of activations into this approach and experiment with more classes of neural networks.

### ACKNOWLEDGEMENTS

The authors would like to thank Marat Dukhan, Bram Wasti and Satish Nadathur for collecting ARM Cortex A-7 and A-75 processor instruction information as well as Misha Smelyanskiy for his helpful comments and suggestions.

---

## REFERENCES

- J. Albericio, P. Judd, T. Hetherington, T. Aamodt, N. E. Jerger, and A. Moshovos. Cnvlutin: Ineffectual-neuron-free deep neural network computing. *ACM/IEEE 43rd Annual International Symposium on Computer Architecture*, 2016.
- H. Bagherinezhad, M. Rastegari, and A. Farhadi. LCNN: Lookup-based convolutional neural network. *Proc. Computer Vision and Pattern Recognition*, 2017.
- Y.H. Chen, T. Krishna, J. Emer, and V. Sze. Eyeriss: An energy-efficient reconfigurable accelerator for deep convolutional neural networks. *IEEE Journal of Solid-State Circuits*, 52:127–138, 2017.
- J. Choi, P. Chuang, Z. Wang, S. Venkataramani, V. Srinivasan, and K. Gopalakrishnan. Bridging the accuracy gap for 2-bit quantized neural networks (QNN). *Proc. Computer Vision and Pattern Recognition*, 2018.
- M. Courbariaux, Y. Bengio, and J.P. David. BinaryConnect: Training deep neural networks with binary weights during propagations. *CoRR*, 2015. URL <https://arxiv.org/abs/1511.00363>.
- M. Courbariaux, I. Hubara, D. Soudry, R. El-Yaniv, and Y. Bengio. Binarized neural networks: Training deep neural networks with weights and activations constrained to +1 or -1. *CoRR*, 2016. URL <https://arxiv.org/abs/1602.02830>.
- J. Deng, W. Dong, R. Socher, L.J. Li, K. Li, and L. Fei-Fei. ImageNet: A large-scale hierarchical image database. *Proc. IEEE Conf. Computer Vision and Pattern Recognition*, pp. 248–255, 2009. URL <http://www.image-net.org>.
- E. Denton, W. Zaremba, J. Bruna, Y. LeCun, and B. Fergus. Exploiting linear structure within convolutional networks for efficient evaluation. *Proc. Neural Information Processing Systems*, 2014.
- A. Devarakonda, M. Naumov, and M. Garland. Adabatch: Adaptive batch sizes for training deep neural networks. *CoRR*, 2017. URL <https://arxiv.org/abs/1712.02029>.
- R. Dolbeau. Theoretical peak flops per instruction set: A tutorial. *The Journal of Supercomputing*, 74:1341–1377, 2018.
- Y. Gong, L. Liu, M. Yang, and L. Bourdev. Compressing deep convolutional networks using vector quantization. *CoRR*, 2014. URL <https://arxiv.org/abs/1412.6115>.
- I. Goodfellow, Y. Bengio, and A. Courville. *Deep Learning*. MIT Press, 2016. URL <https://www.deeplearningbook.org>.
- K. He, X. Zhang, S. Ren, and J. Sun. Deep residual learning for image recognition. *CoRR*, 2015. URL <http://arxiv.org/abs/1512.03385>.
- I. Hubara, M. Courbariaux, D. Soudry, R. El-Yaniv, and Y. Bengio. Quantized neural networks: Training neural networks with low precision weights and activations. *Journal of Machine Learning Research*, 18:1–30, 2018.
- M. Humrick. Exploring DynamIQ and ARM’s new CPUs: Cortex-A75, Cortex-A55. *AnandTech*, 2017. URL <https://www.anandtech.com/show/11441/dynamiq-and-arms-new-cpus-cortex-a75-a55>.
- P. Hung, C. Lee, S. Yang, V. S. Somayazulu, Y. Chen, and S. Chien. Bridge deep learning to the physical world: An efficient method to quantize network. *IEEE Signal Processing Systems*, 2015.
- S. Ioffe and C. Szegedy. Batch normalization: Accelerating deep network training by reducing internal covariate shift. *Proc. International Conf. Machine Learning*, pp. 448–456, 2015. URL <http://proceedings.mlr.press/v37/ioffe15.html>.
- B. Jacob, S. Kligys, B. Chen, M. Zhu, M. Tang, A. Howard, H. Adam, and D. Kalenichenko. Quantization and training of neural networks for efficient integer-arithmetic-only inference. *CoRR*, 2017. URL <https://arxiv.org/abs/1712.05877>.



- 
- M. Jaderberg, A. Vedaldi, and A. Zisserman. Speeding up convolutional neural networks with low rank expansions. *BMVC*, 2014.
- Y. Jia, E. Shelhamer, J. Donahue, S. Karayev, J. Long, R. Girshick, S. Guadarrama, and T. Darrell. Caffe: Convolutional architecture for fast feature embedding. *CoRR*, 2014.
- D. Kim, J. Ahn, and S. Yoo. ZeNA: Zero-aware neural network accelerator. *IEEE Design and Test*, 35:39–46, 2017.
- R. Krishnamoorthi. Quantizing deep convolutional networks for efficient inference: A whitepaper. *CoRR*, 2018.
- A. Krizhevsky, V. Nair, and G. Hinton. CIFAR-10 (Canadian Institute for Advanced Research). 2009. URL <http://www.cs.toronto.edu/~ekriz/cifar.html>.
- A. Krizhevsky, I. Sutskever, and G. E Hinton. ImageNet classification with deep convolutional neural networks. *Advances Neural Information Processing Systems*, pp. 1097–1105, 2012.
- Y. LeCun, B. Boser, J. S. Denker, D. Henderson, R. E. Howard, W. Hubbard, and L. D. Jackel. Backpropagation applied to handwritten zip code recognition. *Neural Computation*, 1:541–551, 1989a.
- Y. LeCun, L. D. Jackel, B. Boser, J. S. Denker, H. P. Graf, I. Guyon, D. Henderson, R. E. Howard, and W. Hubbard. Handwritten digit recognition: Applications of neural net chips and automatic learning. *IEEE Communication*, pp. 41–46, 1989b.
- Y. LeCun, L. Bottou, Y. Bengio, and P. Haffner. Gradient-based learning applied to document recognition. *Proc. IEEE*, 86:2278–2324, 1998. URL <http://yann.lecun.com/exdb/mnist>.
- F. Li, B. Zhang, and B. Liu. Ternary weight networks. *CoRR*, 2016. URL <https://arxiv.org/abs/1605.04711>.
- N. Mellempudi, A. Kundu, D. Mudigere, D. Das, B. Kaul, and P. Dubey. Ternary neural networks with fine-grained quantization. *CoRR*, 2017. URL <https://arxiv.org/abs/1705.01462>.
- S. Migasz. 8-bit inference with Tensor RT. *GTC 2017*. URL <http://on-demand.gputechconf.com/gtc/2017/presentation/s7310-8-bit-inference-with-tensorrt.pdf>.
- A. Mishra and D. Marr. Apprentice: Using knowledge distillation techniques to improve low-precision network accuracy. *CoRR*, 2018. URL <https://arxiv.org/abs/1711.05852>.
- NVIDIA. Turing architecture whitepaper. 2018. URL <https://www.nvidia.com/content/dam/en-zz/Solutions/design-\visualization/technologies/turing-architecture/NVIDIA-Turing-Architecture-Whitepaper.pdf>.
- A. Parashar, M. Rhu, A. Mukkara, A. Puglielli, R. Venkatesan, B. Khailany, J. Emer, S. W. Keckler, and W. J. Dally. SCNN: An accelerator for compressed-sparse convolutional neural networks. *ACM/IEEE 44th Annual International Symposium on Computer Architecture*, 2017.
- E. Park, S. Yoo, and P. Vajda. Value-aware quantization for training and inference of neural networks. *CoRR*, 2018. URL <https://arxiv.org/abs/1804.07802>.
- A. Paszke, S. Gross, S. Chintala, G. Chanan, E. Yang, Z. DeVito, Z. Lin, A. Desmaison, L. Antiga, and A. Lerer. Automatic differentiation in PyTorch. *Proc. Neural Information Processing Systems*, 2017.
- M. Rastegari, V. Ordonez, J. Redmon, and A. Farhadi. XNOR-Net: ImageNet classification using binary convolutional neural networks. *CoRR*, 2016. URL <https://arxiv.org/abs/1603.05279>.

- 
- B. Reagen, P. Whatmough, R. Adolf, S. Rama, H. Lee, S. K. Lee, J. M. Hernandez-Lobato, G.Y. Wei, and D. Brooks. Minerva: Enabling low-power, highly-accurate deep. *ACM/IEEE 43rd Annual International Symposium on Computer Architecture*, 2016.
- A. L. Shimpi. ARM’s Cortex A7: Bringing cheaper dual-core & more power efficient high-end devices. *AnandTech*, 2011. URL <https://www.anandtech.com/show/4991/arms-cortex-a7-bringing-cheaper-dualcore-more-power-efficient/-highend-devices>.
- F. Stenger. Numerical methods based on sinc and analytic functions. *Springer Series in Computational Mathematics*, 20, 1993.
- G. Strang and G. Fix. *An Analysis of the Finite Element Method*. Wellesley-Cambridge Press, 2nd Ed., 2008.
- C. Szegedy, W. Liu, Y. Jia, P. Sermanet, S. Reed, D. Anguelov, D. Erhan, V. Vanhoucke, and A. Rabinovich. Going deeper with convolutions. *CoRR*, 2014. URL <https://arxiv.org/abs/1409.4842>.
- G. Venkatesh, E. Nurvitadhi, and D. Marr. Accelerating deep convolutional networks using low-precision and sparsity. *CoRR*, 2016. URL <https://arxiv.org/abs/1610.00324>.
- P. Wang, Q. Hu, Y. Zhang, C. Zhang, Y. Liu, and J. Cheng. Two-step quantization for low-bit neural networks. *Proc. Computer Vision and Pattern Recognition*, 2018.
- H. Wen, S. Zhou, Z. Liang, Y. Zhang, D. Feng, X. Zhou, and C. Yao. Training bit fully convolutional network for fast semantic segmentation. *CoRR*, 2016. URL <https://arxiv.org/abs/1612.00212>.
- Y. Zhou, S.M. Moosavi-Dezfooli, N.M. Cheung, and P. Frossard. Adaptive quantization for deep neural network. *CoRR*, 2017. URL <https://arxiv.org/abs/1712.01048>.

---

## 5 APPENDIX: BRIEF BACKGROUND

The machine learning models are used in the fields of computer vision (CV) and natural language processing (NLP) among many others. In particular, the deep learning models based on neural networks composed of multiple layers have achieved unprecedented gains in accuracy of image classification and object detection tasks Krizhevsky et al. (2012); Szegedy et al. (2014); LeCun et al. (1998); Krizhevsky et al. (2009); Deng et al. (2009).

In this paper we focus on the CV deep learning models that often rely on convolutional neural networks (CNNs), that are mainly composed of multiple convolution, fully connected and batch normalization layers LeCun et al. (1989a;b); Goodfellow et al. (2016); Ioffe & Szegedy (2015). For example, we will investigate ResNet-20 on CIFAR-10 and ResNet-50 on ImageNet datasets He et al. (2015); Krizhevsky et al. (2009); Deng et al. (2009). For completeness we review the most common layers next.

The convolution layer can be defined as

$$\begin{cases} Z = f(Y) \\ Y = X \odot W \end{cases} \quad (14)$$

where input image  $X \in \mathbb{R}^{h \times w \times c}$ , the filter  $W \in \mathbb{R}^{m \times n \times c}$ , while  $\odot$  denotes a convolution<sup>2</sup> and  $f$  denotes a pooling operation, resulting in output  $Z \in \mathbb{R}^{h' \times w'}$  with  $h' = (h - m)/s_1 + 1$  and  $w' = (w - n)/s_2 + 1$  for strides  $s_1, s_2 \geq 1$ . The operation is usually repeated for  $c'$  output channels, resulting in  $Z \in \mathbb{R}^{h' \times w' \times c'}$ .

The fully connected layer is defined as

$$\begin{cases} Z = f(Y) \\ Y = WX + \mathbf{b}\mathbf{e}^T \end{cases} \quad (15)$$

where input  $X = [\mathbf{x}_1, \dots, \mathbf{x}_r] \in \mathbb{R}^{n \times r}$ , weights  $W \in \mathbb{R}^{m \times n}$ , bias  $\mathbf{b} \in \mathbb{R}^n$ , unit vector  $\mathbf{e}^T = [1, \dots, 1]$ , the non-linear activation function  $f$  is applied component-wise on intermediate  $Y \in \mathbb{R}^{m \times r}$  and output  $Z \in \mathbb{R}^{m \times r}$  for  $r \geq 1$  batch size.

The typical batch normalization layer can be written as

$$\begin{cases} Z = WY + \mathbf{b}\mathbf{e}^T \\ Y = \frac{1}{\sqrt{r}}X(I - \frac{1}{r}\mathbf{e}\mathbf{e}^T) \end{cases} \quad (16)$$

where input  $X = [\mathbf{x}_1, \dots, \mathbf{x}_r] \in \mathbb{R}^{n \times r}$ , scaled diagonal matrix of weights  $W \in \mathbb{R}^{m \times m}$ , bias  $\mathbf{b} \in \mathbb{R}^n$ , unit vector  $\mathbf{e}^T = [1, \dots, 1]$  for  $r \geq 1$  batch size Devarakonda et al. (2017).

---

<sup>2</sup>In this context it is also common to use a cross-correlation rather than a convolution.